

## Original Article



## OPEN ACCESS

**Received:** Jun 30, 2016  
**Revised:** Jul 12, 2016  
**Accepted:** Jul 16, 2016

### Correspondence to Sanghoon Ko

Department of Food Science and Technology,  
Sejong University, 209 Neungdong-ro,  
Gwangjin-gu, Seoul 05006, Korea.  
Tel: +82-2-3408-3260  
Fax: +82-2-3408-4319  
E-mail: sanghoonko@sejong.ac.kr

Copyright © 2016 The Korean Society of  
Clinical Nutrition

This is an Open Access article distributed  
under the terms of the Creative Commons  
Attribution Non-Commercial License (<http://creativecommons.org/licenses/by-nc/3.0/>)  
which permits unrestricted non-commercial  
use, distribution, and reproduction in any  
medium, provided the original work is properly  
cited.

### ORCID

Xiangpeng Meng  
<http://orcid.org/0000-0002-2545-9753>  
Jina Ryu  
<http://orcid.org/0000-0002-7729-2625>  
Bumsik Kim  
<http://orcid.org/0000-0001-8793-7696>  
Sanghoon Ko  
<http://orcid.org/0000-0003-0664-3173>

### Funding

This research was supported by the  
Agriculture Research Center (ARC, 710003-  
03-3-SB120) program of the Ministry for Food,  
Agriculture, Forestry and Fisheries, Korea.

# Application of Iron Oxide as a pH- dependent Indicator for Improving the Nutritional Quality

Xiangpeng Meng,<sup>1</sup> Jina Ryu,<sup>1</sup> Bumsik Kim,<sup>2</sup> Sanghoon Ko<sup>1</sup>

<sup>1</sup>Department of Food Science and Technology, Sejong University, Seoul 05006, Korea

<sup>2</sup>School of Food Science, Kyungil University, Gyeongsan 38428, Korea

## ABSTRACT

Acid food indicators can be used as pH indicators for evaluating the quality and freshness of fermented products during the full course of distribution. Iron oxide particles are hardly suspended in water, but partially or completely agglomerated. The agglomeration degree of the iron oxide particles depends on the pH. The pH-dependent particle agglomeration or dispersion can be useful for monitoring the acidity of food. The zeta potential of iron oxide showed a decreasing trend as the pH increased from 2 to 8, while the point of zero charge (PZC) was observed around at pH 6.0-7.0. These results suggested that the size of the iron oxide particles was affected by the change in pH levels. As a result, the particle sizes of iron oxide were smaller at lower pH than at neutral pH. In addition, agglomeration of the iron oxide particles increased as the pH increased from 2 to 7. In the time-dependent aggregation test, the average particle size was 730.4 nm and 1,340.3 nm at pH 2 and 7, respectively. These properties of iron oxide particles can be used to develop an ideal acid indicator for food pH and to monitor food quality, besides a colorant or nutrient for nutrition enhancement and sensory promotion in food industry.

**Keywords:** Iron oxide; Particle; pH; Acid food indicator

## INTRODUCTION

pH is a basic and important factor in both food processing and food distribution because it affects not only the chemical properties of food materials, but also the status of microbial growth in the internal and external environment of the food system [1-3]. Acid food indicators can be used as pH indicators for evaluating the quality and freshness of fermented food products during the distribution process [4]. Several fruit and vegetable extracts containing pH-responsive pigments such as anthocyanins have been used as edible pH indicators. However, commercial applications of anthocyanin-based acid food indicators have been restricted because they are susceptible to heat, light, pH, oxygen, and some enzymes like polyphenol oxidase.

Iron is a common element existing in the earth and a component of whole living cells [5]. Furthermore, it is an essential trace mineral element for the maintenance of health [6]. However, iron deficiency is still commonly occurring single nutrient deficiency in the world.

### Conflict of Interest

The authors have no potential conflicts of interest to disclose.

### Author Contributions

Xiangpeng Meng drafted the manuscript and tested the physicochemical properties of iron oxide particles. Jina Ryu analyzed the data. Bumsik Kim contributed to interpretation of the results. Sanghoon Ko designed the study, interpreted the results and drafted the manuscript.

Iron-deficiency anemia can be caused by iron loss from the body and insufficient dietary intake or absorption of iron [7]. Iron oxides are widely used in the life (e.g., iron ores, pigments, catalysts, in thermite, hemoglobin) [8,9]. Recently, they are also used as a colorant or nutrient in sausage casings, candies, chewing gums, cosmetics, and some drugs in various industries including the food industry [10]. The use of iron oxides in food is permitted by the General Standard for Food Additives, established by the Codex Committee on Food Additives and Contaminants. One study reported that iron oxide nanoparticles containing nanocomposite films were adopted as a biosensor to indicate glucose levels, but there is no research reporting its application as a pH indicator [11]. Iron oxide is commonly used to produce red color, but its degree of redness is influenced by particle concentration, pH, and other factors [12]. Iron oxide particles are hardly suspended in water; instead, they are partially or completely agglomerated [13]. The degree of iron oxide particle agglomeration varies depending on the pH. The pH-dependent particle agglomeration or dispersion can be useful for indicating acidic foods. This property can be used for indicating carbon dioxide (CO<sub>2</sub>) concentration in foods. A visual indicator reflecting the CO<sub>2</sub> concentration may provide untrained consumers with an efficient and easy way to monitor the quality of foods. Such an indicator is designed to change its appearance depending on the change in pH of the aqueous suspension, due to the equilibrium between dissolved CO<sub>2</sub> and generated carbonic acid [14]. Iron oxide particles in the acidic solution are dispersing, but are getting agglomerating as the pH is increasing up to 7 and above. The change in the agglomeration of iron oxide particles upon H<sup>+</sup> generation from carbonic acid can be utilized as a visual indication system. The mechanism can be largely explained as follows: the amount of H<sup>+</sup> formed from CO<sub>2</sub> dissolved in the food decreases the pH of the suspension containing the iron oxide particles, which leads to the agglomerated particles to gradually disperse under low pH. Previous studies have reported the application of an indication system based on the variation of pH in smart packaging [15-17]. For this reason, iron oxide particles in the suspension can be used to detect the quality of food depending on the CO<sub>2</sub> concentration. **Figure 1** gives a brief illustration of this mechanism. Hilty [18] reported that nanostructured iron oxide can improve the solubility of iron in the acids and the sensory characteristics in foods. In addition, many of previous studies proved that antibacterial activity of iron oxide nanoparticles can be used against microbe such as *Escherichia coli* [19]. Dietary iron oxide nanoparticles can have the function to delay the neurodegeneration and aging in drosophila [20]. All these previous reports can certificate that iron oxide is safe as a food additive and has the bio containment in microbiome or other organisms.

The objectives of this study were to determine the physicochemical properties of iron oxide particles and to investigate their potential use as a visual indicator for acid, acidified, and fermented foods.

## MATERIALS AND METHODS

### Materials

Iron (III) oxide MP 99.9% (< 10 μm) was purchased from American Elements, USA. Extra pure grade disodium hydrogen phosphate anhydrous (Na<sub>2</sub>HPO<sub>4</sub>) and sodium dihydrogen phosphate (NaH<sub>2</sub>PO<sub>4</sub>) were obtained from Daejung Chemical Co., Korea. Sodium citrate, citric acid, bile extract, lipase, pancreatin, and sodium bicarbonate (NaHCO<sub>3</sub>) were obtained from Sigma-Aldrich, USA.

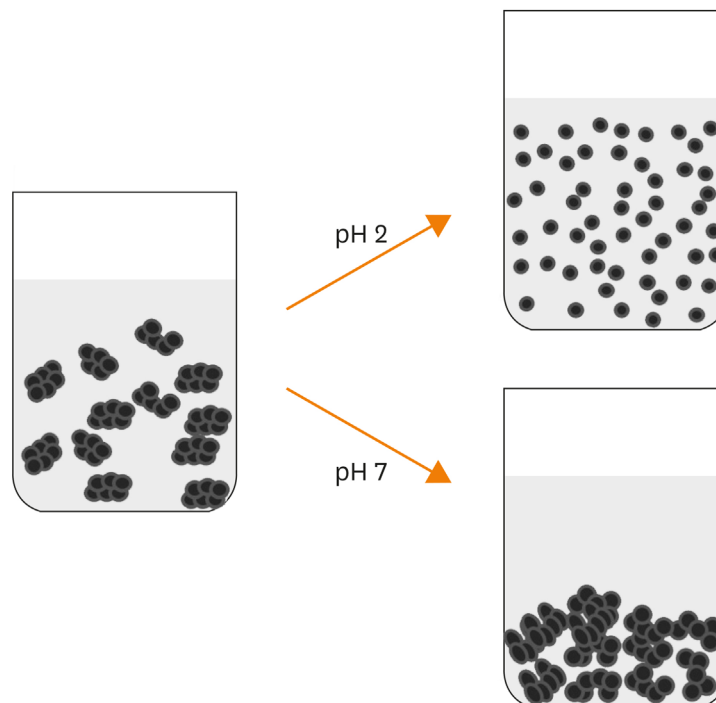


**Figure 1.** Illustration of the indication process of iron nanoparticles as CO<sub>2</sub> indicator at pH 2 and pH 7 condition.

### Scanning electron microscopy (SEM)

The iron oxide MP 99.9% (< 10 μm) was examined using a field-emission scanning electron microscope (FE-SEM, S-4300, Hitachi, Tokyo, Japan) to verify its size. An accelerating voltage of 15.0 kV was used for each sample.

### Particle size distribution measurement

Particle size distribution was determined on a particle size analyzer (Delsa Nano C, Beckman Coulter, Inc., Fullerton, CA, USA) using the dynamic light scattering (DLS) method. Fe<sub>2</sub>O<sub>3</sub> powder (0.1 g) was suspended in 100 mL of deionized water and stirred using a magnetic stirrer (Wisestir MS-MP4, DAIHAN Scientific Co., Ltd., Seoul, Korea) at room temperature, 500 rpm for 1 hour. The suspended sample was then subjected to sonication using an ultrasonic processor (VCX-750, Sonics & Materials, Newtown, CT, USA) at 38% power using a 6 mm diameter probe for 20 minutes. After the sample was pre-treated, the mean diameters of the particles were measured on an intensity basis using the particle size analyzer. The suspension was poured into a cuvette and its particle size was measured at 25°C with a fixed scattering angle of 165°. Each sample was analyzed at least three times.

### Zeta potential at different pH levels

The zeta potential was measured using a particle size analyzer using the electrophoretic light scattering method. Samples were diluted 10 fold using deionized water. The pH was then adjusted to 2.0, 4.0, 6.0, 8.0, 10.0, and 12.0 with either HCl or NaOH. Subsequently, 1 mL of the pH-adjusted sample was injected into a flow cell. The zeta potential was measured at five points in the cell, viz. 0.7, 0.35, 0, -0.35, and -0.7. All samples were measured three times at a fixed temperature and angle of 25°C and 15°, respectively.

### Time-dependent agglomeration at different pH levels

Time-dependent agglomeration of the iron (III) oxide particles was measured by the particle size analyzer using the DLS method. For time-dependent aggregation of iron (III) oxide at pH 2.0 and 7.0, the change in particle size was measured at 37°C for 1 hour with 2 seconds intervals.

### Statistics

All data were measured three times and the processing of original data and graphs are operated by the Simplot 10.0 version (Systat Software, Inc., San Jose, CA, USA).

## RESULTS

### Physicochemical properties of iron oxide powder by scanning electron microscopy

A typical SEM micrograph clearly shows the three-dimensional shape of the iron oxide powders, illustrating the surface morphology of the iron oxide particles (Figure 2). The iron oxide particles had a stable and common structure. The SEM image shows the nanoscale particles with estimated particle size ranging from 200 to 250 nm, indicating the inhomogeneity in particle size distribution. The iron oxide particles showed agglomerated and clustered morphology. The size distribution of the iron oxide particles was measured using DLS, as shown in Figure 3. The average size of the iron oxide particles was approximately 300 nm.

### Zeta potentials of iron oxide at different pH levels

The zeta potentials of iron oxide at different pH values are shown in Figure 4. Zeta potential indicates the dispersion stability of particles in colloids. The zeta potentials of the iron oxides were varied in the range between 32.5 mV to -19.4 mV. The zeta potential of the iron oxides showed a decreasing trend when the pH increased from 2 to 8, while PZC was observed around at pH 6-7. These results suggested that particle aggregation would occur when the pH was close to neutral.

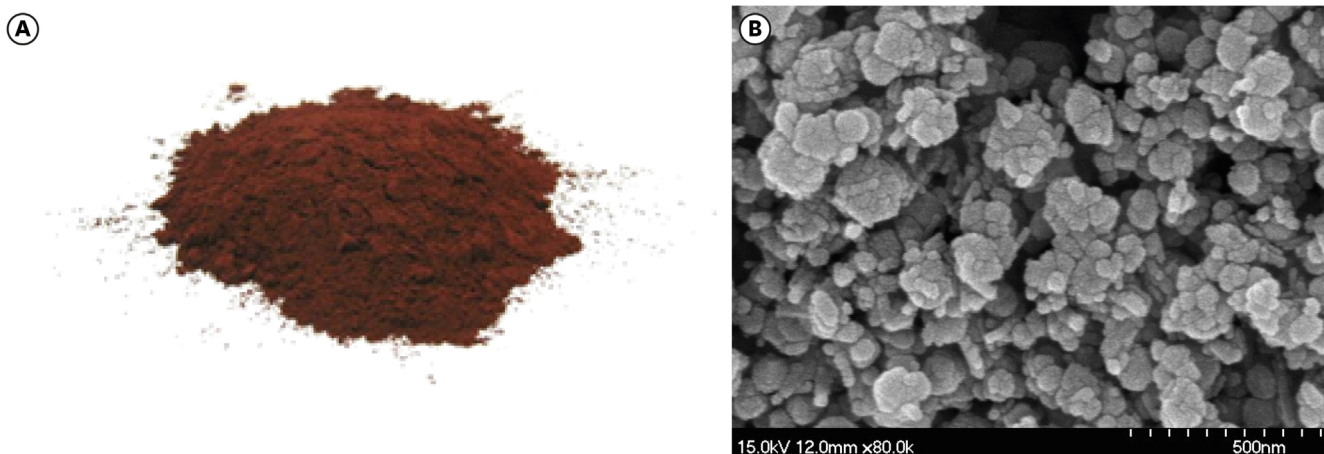


**Figure 2.** Picture of iron oxide particles.

(A) Normal graph of iron oxide powder by naked eye, (B) Micrographs of iron oxide particles by SEM (scale bars, from left to right: 500 nm).

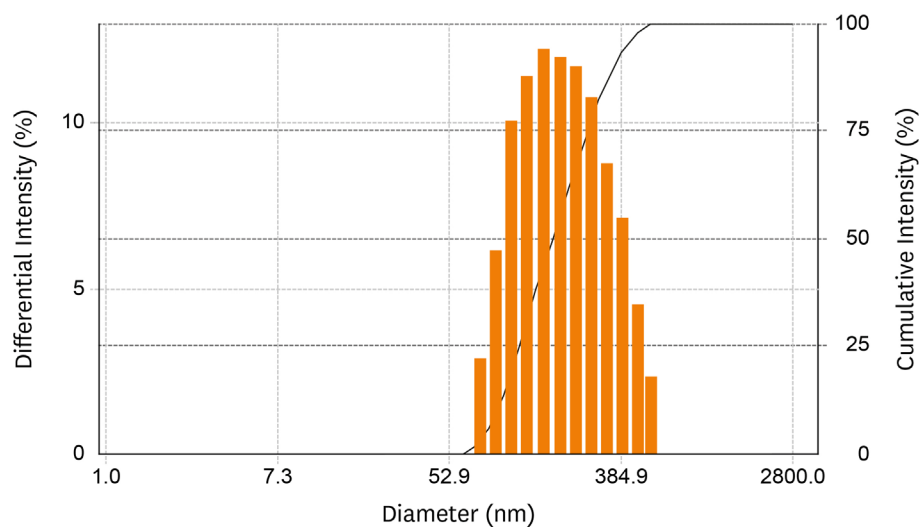


Figure 3. Size distribution of iron oxide particles.

### Time-dependent aggregation at different pH levels

The changes in the particle size of iron oxide at different pH levels are shown in Figure 5. The initial particle size at pH 2.0 was 446.5 nm and the particle sizes were varied between 315.6 nm and 1,295.6 nm overtime. The average particle size was 730.4 nm. The initial particle size at pH 7.0 was 1,440.5 nm and the particle sizes were varied between 1,101.4 nm and 1,496.5 nm. The average particle size was 1,340.3 nm. These results confirmed that the pH level affects the size of the metal oxide particles. At pH 2.0, the suspension was stable and no precipitation was observed, while precipitation was gradually observed at pH values close to 7. These results also proved that the size of the nanoparticles depends on the pH. Thus, lower pH values result in a smaller particle size of iron oxide [21-23] which can be an important factor for developing an acid indicator.

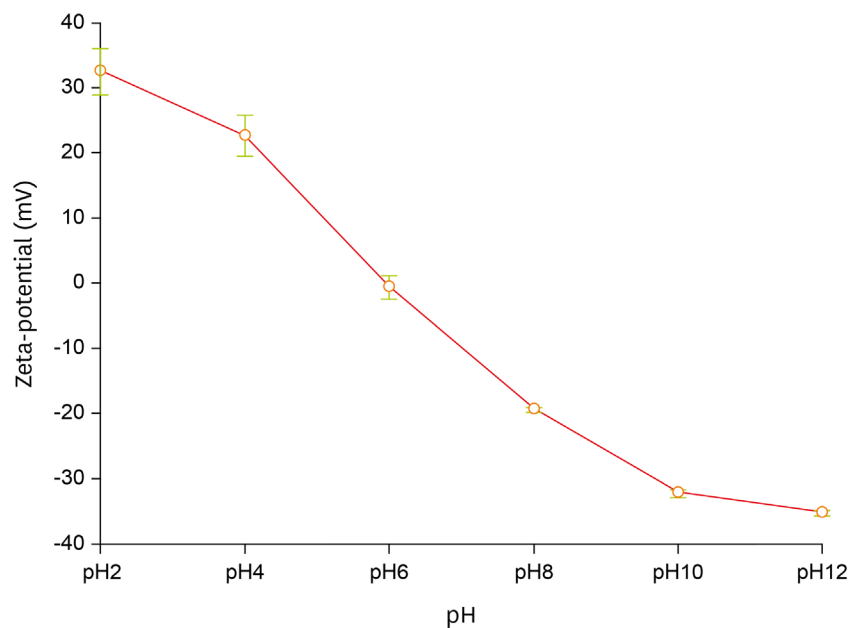


Figure 4. Zeta-potential of iron oxide particles at different pH levels.

## DISCUSSION

DLS values of the iron oxide particles showed that the particles were aggregated in water and their particle sizes were larger than the primary nanoparticle size (100 nm) obtained from the SEM images. Thus, the average particle size was slightly greater than the size determined via SEM because the particles were agglomerated when iron oxide powder was dispersed in distilled water [24]. Zeta potential measurement of the iron oxides showed that the PZC of the iron oxides was around at pH 6.0-7.0. These results confirmed that particle aggregation would occur when the pH was close to neutral. At zeta potential ranging from 0 to  $\pm 5$  mV, the suspension was so unstable that the particles could be rapidly agglomerated or coagulated. However, the zeta potential of iron oxide at pH 2 was higher than that at pH 7.0. Generally, particles with zeta potential greater than  $\pm 30$  mV were moderately stable, whereas particles with zeta potential less than  $\pm 30$  mV showed an incipient settling. This pH-based aggregation is ideal for adoption in an acid indicator for pH indication in food systems. As indicated in previous studies, different pH levels affected the degree of aggregation, stabilization, and bioavailability of the nanoparticles [25,26]. This phenomenon involves a gradual variation and therefore, it can be useful for making potential food indicators to monitor the nutritional quality and safety of acidic foods during the food processing and distribution. Furthermore, iron oxides are widely applied in clinical nutrition and treatment field, for example, in constructing the drug delivery system, they are used as carriers in magnetic drug targeting for cancer treatment and other application such as tissue repair, and coating of polymer and protein and so on [23,27,28]. In addition, iron deficiency is still considered the most common single nutrient deficiency in the world. Therefore, this study result suggests beneficial information on the research for iron-fortified foods and pharmaceuticals.

## CONCLUSION

The agglomeration grade and particle size of iron oxide particles were affected by the pH levels. The particles size was smaller at lower pH than at neutral pH, because agglomeration increased when the pH changed from 2.0 to 7.0. This is attributed to the pH-dependent zeta

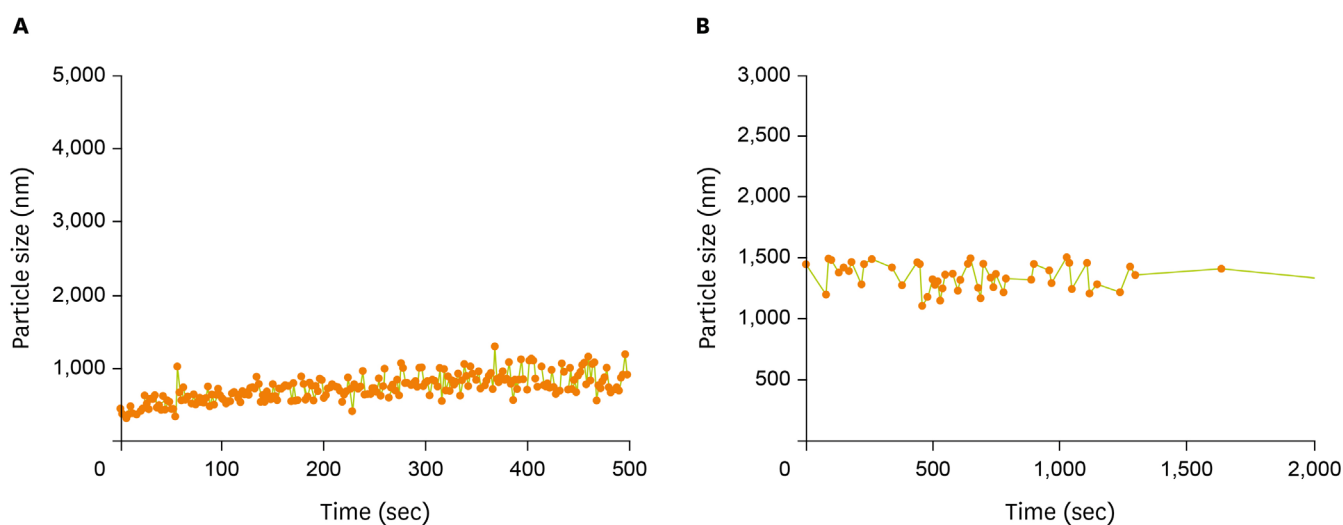


**Figure 5.** Time-resolved DLS of iron oxide particle suspensions at different pH: (A) pH 2.0 and (B) pH 7.0.

potential variation of the iron oxide particles. This mechanism can be used to develop an ideal acid indicator for monitoring the food pH and quality through the agglomeration or dispersion of iron oxide particles depending on the pH. In addition, iron oxide is also a kind of colorant or nutrient that is used for nutrition enhancement and sensory promotion in the food industry. Further studies are therefore necessary to investigate the linear relationship between particle agglomeration and factors such as CO<sub>2</sub> concentration, acid generation, and microbial growth, all of which can affect the pH of food systems. Also, another further study is needed to use food matrix to validate these results and to test consumer acceptability by sensory evaluation.

## REFERENCES

1. Fontoin H, Saucier C, Teissedre PL, Glories Y. Effect of pH, ethanol and acidity on astringency and bitterness of grape seed tannin oligomers in model wine solution. *Food Qual Prefer* 2008;19:286-91.  
[CROSSREF](#)
2. Wismer-Pedersen J. Quality of pork in relation to rate of pH change post mortem. *J Food Sci* 1959;24:711-27.  
[CROSSREF](#)
3. Gibson AM, Bratchell N, Roberts TA. Predicting microbial growth: growth responses of salmonellae in a laboratory medium as affected by pH, sodium chloride and storage temperature. *Int J Food Microbiol* 1988;6:155-78.  
[PUBMED](#) | [CROSSREF](#)
4. Hong SI, Park WS. Use of color indicators as an active packaging system for evaluating kimchi fermentation. *J Food Eng* 2000;46:67-72.  
[CROSSREF](#)
5. Neilands JB. Iron absorption and transport in microorganisms. *Annu Rev Nutr* 1981;1:27-46.  
[PUBMED](#) | [CROSSREF](#)
6. Mertz W. The essential trace elements. *Science* 1981;213:1332-8.  
[PUBMED](#) | [CROSSREF](#)
7. Booth IW, Aukett MA, Logan S. Iron deficiency anaemia in infancy and early childhood. *Arch Dis Child* 1997;76:549-53.  
[PUBMED](#) | [CROSSREF](#)
8. Neves MC, Pascoal Neto C, Trindade T. Eco-friendly hybrid pigments made of cellulose and iron oxides. *J Nanosci Nanotechnol* 2012;12:6817-21.  
[PUBMED](#) | [CROSSREF](#)
9. Shimojo F, Nakano A, Kalia RK, Vashishta P. Electronic processes in fast thermite chemical reactions: a first-principles molecular dynamics study. *Phys Rev E Stat Nonlin Soft Matter Phys* 2008;77:066103.  
[PUBMED](#) | [CROSSREF](#)
10. Chaudhry Q, Castle L. Food applications of nanotechnologies: an overview of opportunities and challenges for developing countries. *Trends Food Sci Technol* 2011;22:595-603.  
[CROSSREF](#)
11. Baalousha M. Aggregation and disaggregation of iron oxide nanoparticles: influence of particle concentration, pH and natural organic matter. *Sci Total Environ* 2009;407:2093-101.  
[PUBMED](#) | [CROSSREF](#)
12. Chan T, Verma MS, Gu FX. Optimization of polydiacetylene-coated superparamagnetic magnetite biosensor for colorimetric detection of biomarkers. *J Nanosci Nanotechnol* 2015;15:2628-33.  
[PUBMED](#) | [CROSSREF](#)
13. Morillo D, Pérez G, Valiente M. Efficient arsenic(V) and arsenic(III) removal from acidic solutions with Novel Forager Sponge-loaded superparamagnetic iron oxide nanoparticles. *J Colloid Interface Sci* 2015;453:132-41.  
[PUBMED](#) | [CROSSREF](#)
14. Meng X, Lee K, Kang TY, Ko S. An irreversible ripeness indicator to monitor the CO<sub>2</sub> concentration in the headspace of packaged kimchi during storage. *Food Sci Biotechnol* 2015;24:91-7.  
[CROSSREF](#)
15. Jung J, Puligundla P, Ko S. Proof-of-concept study of chitosan-based carbon dioxide indicator for food packaging applications. *Food Chem* 2012;135:2170-4.  
[PUBMED](#) | [CROSSREF](#)



16. Lee K, Meng X, Kang TY, Ko S. A dye-incorporated chitosan-based CO<sub>2</sub> indicator for monitoring of food quality focusing on makgeolli quality during storage. *Food Sci Biotechnol* 2015;24:905-12.  
[CROSSREF](#)
17. Jung J, Lee K, Puligundla P, Ko S. Chitosan-based carbon dioxide indicator to communicate the onset of kimchi ripening. *Lebensm Wiss Technol* 2013;54:101-6.  
[CROSSREF](#)
18. Hilty FM, Knijnenburg JT, Teleki A, Krumeich F, Hurrell RF, Pratsinis SE, Zimmermann MB. Incorporation of Mg and Ca into nanostructured Fe<sub>2</sub>O<sub>3</sub> improves Fe solubility in dilute acid and sensory characteristics in foods. *J Food Sci* 2011;76:N2-10.
19. Gordon T, Perlstein B, Houbara O, Felner I, Banin E, Margel S. Synthesis and characterization of zinc/iron oxide composite nanoparticles and their antibacterial properties. *Colloids Surf A Physicochem Eng Asp* 2011;374:1-8.  
[CROSSREF](#)
20. Zhang Y, Wang Z, Li X, Wang L, Yin M, Wang L, Chen N, Fan C, Song H. Dietary iron oxide nanoparticles delay aging and ameliorate neurodegeneration in drosophila. *Adv Mater* 2016;28:1387-93.  
[PUBMED](#) | [CROSSREF](#)
21. Saleh N, Kim HJ, Phenrat T, Matyjaszewski K, Tilton RD, Lowry GV. Ionic strength and composition affect the mobility of surface-modified FeO nanoparticles in water-saturated sand columns. *Environ Sci Technol* 2008;42:3349-55.  
[PUBMED](#) | [CROSSREF](#)
22. Navrotsky A, Mazeina L, Majzlan J. Size-driven structural and thermodynamic complexity in iron oxides. *Science* 2008;319:1635-8.  
[PUBMED](#) | [CROSSREF](#)
23. Gupta AK, Gupta M. Synthesis and surface engineering of iron oxide nanoparticles for biomedical applications. *Biomaterials* 2005;26:3995-4021.  
[PUBMED](#) | [CROSSREF](#)
24. Zhang Y, Chen Y, Westerhoff P, Hristovski K, Crittenden JC. Stability of commercial metal oxide nanoparticles in water. *Water Res* 2008;42:2204-12.  
[PUBMED](#) | [CROSSREF](#)
25. Domingos RF, Tufenkji N, Wilkinson KI. Aggregation of titanium dioxide nanoparticles: role of a fulvic acid. *Environ Sci Technol* 2009;43:1282-6.  
[PUBMED](#) | [CROSSREF](#)
26. French RA, Jacobson AR, Kim B, Isley SL, Penn RL, Baveye PC. Influence of ionic strength, pH, and cation valence on aggregation kinetics of titanium dioxide nanoparticles. *Environ Sci Technol* 2009;43:1354-9.  
[PUBMED](#) | [CROSSREF](#)
27. Berry CC, Curtis AS. Functionalisation of magnetic nanoparticles for applications in biomedicine. *J Phys D Appl Phys* 2003;36:R198-206.  
[CROSSREF](#)
28. Chomoucka J, Drbohlavova J, Huska D, Adam V, Kizek R, Hubalek J. Magnetic nanoparticles and targeted drug delivering. *Pharmacol Res* 2010;62:144-9.  
[PUBMED](#) | [CROSSREF](#)